

Band structures in ^{132}Ba

S. Juutinen,¹ S. Törmänen,¹ P. Ahonen,¹ M. Carpenter,^{2,*} C. Fahlander,³ J. Gascon,^{2,†} R. Julin,¹ A. Lampinen,¹ T. Lönnroth,⁴ J. Nyberg,^{2,3} A. Pakkanen,¹ M. Piiparinen,¹ K. Schiffer,² P. Šimeček,⁵ G. Sletten,² and A. Virtanen¹

¹*Department of Physics, University of Jyväskylä, P.O. Box 35, FIN-40351 Jyväskylä, Finland*

²*Tandem Accelerator Laboratory, Niels Bohr Institute, DK-4000 Roskilde, Denmark*

³*The Svedberg Laboratory, University of Uppsala, Box 535, S-75121 Uppsala, Sweden*

⁴*Department of Physics, Åbo Akademi, FIN-20500 Turku, Finland*

⁵*Institute of Nuclear Physics, Czech Academy of Sciences, 25068 Rez near Prag, Czech Republic*

(Received 16 August 1995)

Excited states of ^{132}Ba were studied in an experiment utilizing the $^{124}\text{Sn}(^{13}\text{C},5n)$ reaction at a beam energy of 65.5 MeV. The level scheme of ^{132}Ba was considerably extended from what was previously known. Evidence is presented for neutron $h_{11/2}$ alignments, which are predicted to drive the nucleus to a shape with $\gamma \approx -80^\circ$. Two strongly coupled $\Delta I=1$ bands were also observed.

PACS number(s): 21.10.Re, 23.20.Lv, 27.60.+j

I. INTRODUCTION

Nuclei in the transitional region $Z \geq 50$ and $N \leq 82$ are of interest because they show a large variety of coexisting structures. The nucleus ^{132}Sn and nuclei close to this core nucleus exhibit clear shell-model structures [1,2]. On the other hand, well-developed band structures are found in, e.g., the Sb isotopes ($Z=51$) at higher excitation energies and also very prominent “intruder bands” based on proton particle-hole excitations are observed [3–5]. These intruder structures are still found in odd- A iodine isotopes with $Z=53$ [6]. In Te and Xe isotopes with $Z=52$ and 54, vibrational-like bands and two-quasiparticle excitations coexist. In ^{132}Xe the “typical” two-quasineutron sequence of this region with $I^\pi=5^-, 7^-,$ and 10^+ states is well established. The 10^+ state is a long-lived isomer with $T_{1/2}=8.4$ ms [7].

The more proton-rich nuclei, like Ba ($Z=56$) or Ce ($Z=58$), seem to develop a clear rotational structure in the light isotopes. However, even in the cerium isotopes the neutron–two-quasiparticle excitations seem to be yrast in the close neighborhood of the $N=82$ shell closure, as has been demonstrated in $^{134}\text{Ce}_{78}$ [8,9]. Thus, in the transitional $^{132-134}\text{Ba}$ isotopes one could expect coexistence of these two excitations with a possibility of interesting interplay between them. Also in ^{134}Ba the $5^-, 7^-,$ and 10^+ states are observed [10] and they are isomeric, whereas in ^{130}Ba the states clearly start to form (collective) band structures [11].

One of the interesting properties of the nuclei in this mass region is that several even-even nuclei show two S bands corresponding to aligned neutron and proton $h_{11/2}^2$ configurations. In the light Ba isotopes, which are well deformed, the

lower S band is attributed to the proton $h_{11/2}^2$ configuration [12,13]. In the heavier Ba isotopes with decreasing quadrupole deformation and more negative γ deformation, the neutron S band becomes favored. In ^{132}Ba the observed S band is associated with the neutron $h_{11/2}^2$ configuration [14]. The systematics of the S bands in Xe, Ba, and Ce nuclei has been discussed in [15]. For the nuclei around ^{132}Ba , the proton Fermi level is just below the low- Ω orbitals originating from the $h_{11/2}$ shell, while the neutron Fermi level is close to the top of the $h_{11/2}$ shell. This results in very different shape driving tendencies of protons and neutrons: The proton and neutron $h_{11/2}$ configurations favor shapes with $\gamma > 0^\circ$ and $\gamma < -60^\circ$, respectively.

The present work aims at studying the excited structures of the transitional $Z=50+6$ nucleus ^{132}Ba having $N=76$. A previous study using ^{13}C induced reactions has revealed several high-spin bands in ^{132}Ba [14]. In the present work employing the NORDBALL detector array new sidebands were found.

II. EXPERIMENTAL PROCEDURE AND RESULTS

Excited states in ^{132}Ba were populated by bombarding a ^{124}Sn target with a ^{13}C beam. The ^{13}C beam was provided by the tandem accelerator of the Niels Bohr Institute in Denmark. The γ rays were detected in the multidetector facility NORDBALL [16] consisting of 15 Compton-suppressed Ge detectors and a ten-element BaF_2 multiplicity filter. The target consisted of a 1.7 mg/cm^2 thick layer of ^{124}Sn enriched to 97.5% on an 11 mg/cm^2 thick gold backing. A beam energy of 65.5 MeV was used producing mainly ^{132}Ba and ^{133}Ba via the $(^{13}\text{C},5n)$ and $(^{13}\text{C},4n)$ reaction channels, respectively. About 10^8 $\gamma\gamma$ -coincidence events were collected with the condition that at least two Ge detectors and one element of the multiplicity filter fired.

The γ rays attributed to ^{132}Ba in this experiment, together with their intensities and placements, are listed in Table I. The spin assignments rely on the $R=I_\gamma(37^\circ)$ or

*Present address: Argonne National Laboratory, Argonne, IL 60439-4843.

†Present address: Laboratoire de Physique Nucléaire, Université de Montréal, C.P. 6128, Montréal, Québec, Canada H3C 3J7.

TABLE I. The γ -ray energies, intensities, and $R = I_\gamma(37^\circ \text{ or } 143^\circ)/I_\gamma(79^\circ \text{ or } 101^\circ)$ angular distribution ratios for the transitions assigned to ^{132}Ba .

E_γ^a	I_γ	R^b	Spin assignment	Band
125.5	4.0(6)	0.50(7)	$7^- \rightarrow 6^-$	5→6
151.9	0.38(7)	1.06(10)	$9^- \rightarrow 9^-$	10→5
169.9	2.7(2)	0.73(5)	$15^- \rightarrow 14^-$	9
175.3	0.70(5)	0.58(8)	$5^- \rightarrow 4^-$	5→6
185.4	0.40(5)	0.82(8)	$12^+ \rightarrow 11^+$	3
187.7	1.2 (1)	0.79(5)	$5^- \rightarrow 6^+$	5→yrast
203.9	1.8(1)	0.76(3)	$13^+ \rightarrow 12^+$	3
215.7	5.0(3)	0.75(3)	$16^- \rightarrow 15^-$	9
229.0	0.70(5)	0.65(7)	$11^- \rightarrow 10^-$	10→11
235.2	1.3(2)	0.71(6)	$9^- \rightarrow 8^-$	10→11
235.9	2.3(2)	0.72(4)	$14^+ \rightarrow 13^+$	3
236.1	0.7(2)	0.73(7)	$16^- \rightarrow 15^-$	9→
238.1	7.4(4)	0.55(3)	$6^- \rightarrow 5^-$	6→5
242.5	5.5(3)	0.78(4)	$7^- \rightarrow 6^+$	5→ γ
245.5	0.60(5)	0.40(8)	$9^- \rightarrow 8^-$	10→7
249.1	1.5(1)	1.39(11)	$10^+ \rightarrow 8^+$	yrast→ γ
275.3	0.80(8)	0.66(5)	$14^+ \rightarrow 13^+$	→3
285.6	3.0(2)	0.72(7)	$5^- \rightarrow 4^-$	8→7
287.7	1.3(1)	0.66(5)	$9^- \rightarrow 8^-$	5→6
295.4	0.90(6)	0.45(4)	$15^+ \rightarrow 14^+$	3→
295.6	1.1(1)	0.43(4)	$7^- \rightarrow 6^-$	8→7
296.0	0.4(1)		$16^+ \rightarrow 15^+$	yrast→1
297.6	0.3(1)	0.84(8)	$5^- \rightarrow 4^+$	7→ γ
303.1	4.0(2)	0.65(3)	$6^- \rightarrow 5^-$	7→5
307.7	3.5(2)	0.72(5)	$17^- \rightarrow 16^-$	9
316.0	36(2)	1.39(2)	$10^+ \rightarrow 8^+$	yrast
317.0	0.5(1)		$18^+ \rightarrow 17^+$	yrast→1
330.7	0.9(1)		$6^- \rightarrow 4^-$	6→7
335.0	2.3(2)	0.62(4)	$15^+ \rightarrow 14^+$	3
360.5	0.81(5)	0.75(6)	$7^- \rightarrow 6^-$	8→6
363.5	19.5(10)	1.46(3)	$7^- \rightarrow 5^-$	5
376.5	1.2(1)	0.57(5)	$8^- \rightarrow 7^-$	7→8
378.1	0.80(7)	0.54(9)	$17^- \rightarrow 16^-$	10→9
381.1	0.60(5)	0.62(4)	$10^- \rightarrow 9^-$	11→10
383.0	0.20(4)		$3^+ \rightarrow 4^+$	γ →yrast
383.0	0.40(5)	0.68(7)	$(9^+) \rightarrow (8^+)$	
386.6	0.70(6)	0.51(4)	$8^- \rightarrow 7^-$	11→8
387.6	0.33(5)		$9^- \rightarrow 8^-$	8→7
390.3	20.0(10)	0.73(3)	$5^- \rightarrow 4^+$	5→ γ
395.7	3.1(2)	1.5(2)	$6^- \rightarrow 4^-$	7
402.1	0.91(14)	0.69(8)	$11^- \rightarrow 10^-$	5→6
406.9	1.3(1)	0.66(7)	$18^- \rightarrow 17^-$	9
417.5	6.0(3)	0.43(4)	$8^- \rightarrow 7^-$	6→5
424.6	2.2(2)	0.56(4)	$16^+ \rightarrow 15^+$	3
438.4	1.5(2)	1.32(8)	$9^- \rightarrow 7^-$	10
439.5	0.90(10)	0.39(3)	$9^- \rightarrow 8^-$	10→6
455	0.68(6)	0.61(5)	$15^+ \rightarrow 14^+$	1→ γ
455.5	1.0(2)	0.46(4)	$9^- \rightarrow 8^-$	→6
462.4	8.3(4)	1.34(6)	$15^- \rightarrow 13^-$	5
464.6		1.19(2)	$2^+ \rightarrow 0^+$	yrast
466	<0.5		$(19^-) \rightarrow 18^-$	9
469	<0.5		$(17^+) \rightarrow 16^+$	3
470.8	0.90(6)	0.60(2)	$10^- \rightarrow 9^-$	6→5
477.8	1.7(2)	1.25(7)	$8^- \rightarrow 6^-$	6→7

TABLE I. (Continued).

E_γ ^a	I_γ	R ^b	Spin assignment	Band
479	0.5(1)		(18 ⁺)→(17 ⁺)	3
479.3	2.0(2)		3 ⁺ →2 ⁺	γ
490.2	0.60(6)	0.72(7)	12 ⁻ →11 ⁻	11→10
494.6	<0.2		12 ⁻ →11 ⁻	6→5
511.3	5.2(3)	1.40(7)	6 ⁺ →4 ⁺	γ
516.2	3.8(2)	0.85(8)	4 ⁻ →3 ⁺	7→ γ
537.8	1.5(1)	0.62(6)	17 ⁺ →16 ⁺	1→yrast
540.0	2.1(1)	0.77(5)	9 ⁻ →8 ⁺	10→yrast
542.8	0.45(7)	1.2(2)	6 ⁻ →4 ⁻	6
547	0.3(1)		13 ⁻ →12 ⁻	→6
551.3	1.0(1)	0.63(6)	7 ⁻ →6 ⁺	5→yrast
559.5	2.6(2)	1.35(9)	8 ⁺ →6 ⁺	yrast→ γ
567.4	12.3(7)	0.95(4)	2 ⁺ →2 ⁺	γ →yrast
593.7	0.34(6)		11 ⁻ →9 ⁻	10→
598.7	5.1(3)	1.39(6)	7 ⁻ →5 ⁻	8→5
601.7	6.3(4)	0.80(4)	4 ⁺ →4 ⁺	γ →yrast
603.4	1.5(1)	1.40(14)	8 ⁻ →6 ⁻	→6
608	0.3(1)		15 ⁻ →15 ⁻	9→5
610.2	10.0(5)	1.39(6)	11 ⁻ →9 ⁻	10
616.5	1.9(1)	1.51(14)	10 ⁻ →8 ⁻	11
621.8	1.3(1)	0.62()	8 ⁻ →7 ⁻	11→5
622.1	2.3(2)		9 ⁻ →7 ⁻	10→8
624.8	0.37(5)		14 ⁻ →13 ⁻	11→10
626.2	1.3(1)		8 ⁺ →6 ⁺	γ
626.7	1.2(1)	1.5(2)	10 ⁻ →8 ⁻	11→7
630.9	0.60(8)	1.37(13)	12 ⁺ →12 ⁺	→yrast
663.3	100	1.26(2)	4 ⁺ →2 ⁺	yrast
671.4	1.3(2)	1.43(12)	14 ⁺ →12 ⁺	4
672.0	1.5(1)	1.4(2)	8 ⁻ →6 ⁻	7
682.1	1.5(2)	1.4(2)	8 ⁻ →6 ⁻	11→7
683.8	1.3(1)	1.5(2)	12 ⁺ →10 ⁺	γ
686.4	0.7(2)	1.3(2)	14 ⁺ →12 ⁺	4
697.9	16.8(9)	1.35(2)	4 ⁺ →2 ⁺	γ
705.2	16.3(9)	1.36(3)	9 ⁻ →7 ⁻	5
708.3	1.2(2)	0.45(6)	16 ⁻ →15 ⁻	6→5
709.1	0.60(10)		(7 ⁺)→(5 ⁺)	γ
715.2	1.6(2)		(5 ⁺)→3 ⁺	γ
716.2 ^c	0.8(2)	1.13(12)		
719.0	2.9(2)	1.16(9)	12 ⁻ →10 ⁻	11
723.3	0.55(5)	1.43(13)	14 ⁺ →12 ⁺	γ
724	0.16(4)		→(9 ⁺)	
731.8	1.1(2)	1.3(2)	10 ⁺ →8 ⁺	2→ γ
734.6	2.9(2)	0.46(3)	15 ⁺ →14 ⁺	1→yrast
737.2	0.75(9)	1.5(3)	8 ⁻ →6 ⁻	7→6
745.4	0.8(1)	0.85(8)	9→8 ⁺	→yrast
747.3	1.0(1)	1.4(2)	8 ⁻ →6 ⁻	11→6
758.4	8.6(5)	1.40(4)	13 ⁻ →11 ⁻	5
758.7	4.8(3)	1.41(5)	10 ⁻ →8 ⁻	6
761.1	8.2(5)	1.36(4)	13 ⁻ →11 ⁻	10
763	0.8(2)	1.3(2)	12 ⁺ →10 ⁺	γ →2
764.0	1.5(2)	1.3(2)	9 ⁻ →7 ⁻	8
764.4	0.79(8)	1.4(2)	14 ⁻ →12 ⁻	6
783.1	1.0(1)	0.39(5)	12 ⁺ →11 ⁺	4→
789.9	5.0(3)	0.39(4)	11 ⁺ →10 ⁺	→yrast
798.3	1.2(2)	0.39(14)	12 ⁺ →11 ⁺	4→

TABLE I. (Continued).

E_γ ^a	I_γ	R ^b	Spin assignment	Band
798.6	4.4(4)		$10^+ \rightarrow 8^+$	2 \rightarrow yrast
799.6	30.0(15)	1.37(3)	$12^+ \rightarrow 10^+$	yrast
804.2	64(4)	1.29(3)	$6^+ \rightarrow 4^+$	yrast
810.9	3.7(2)	1.22(6)	$10^+ \rightarrow 8^+$	γ
817.0	1.0(1)		$4^- \rightarrow 4^+$	6 \rightarrow yrast
828.5 ^c	1.2(2)			
834.9	0.90(7)	1.4(2)	$17^+ \rightarrow 15^+$	1
837.4	1.2(1)	1.26(13)	$15^- \rightarrow 13^-$	
840.2	1.0(2)		$17^- \rightarrow 15^-$	9 \rightarrow 10
855.0	1.0(2)	1.3(2)	$18^+ \rightarrow 16^+$	yrast
857.3	1.7(3)	1.31(8)	$9^- \rightarrow 7^-$	10 \rightarrow 5
857.6	1.6(1)	1.32(11)	$15^- \rightarrow 13^-$	9 \rightarrow
862.7	5.9(3)	1.32(7)	$15^- \rightarrow 13^-$	10
868.3	48(3)	1.29(3)	$8^+ \rightarrow 6^+$	yrast
871.7	0.8(2)	1.6(2)	$14^+ \rightarrow 12^+$	3 \rightarrow 2
873.1	13.7(7)	1.36(4)	$11^- \rightarrow 9^-$	5
880.5	0.40(5)	1.5(2)	$14^- \rightarrow 12^-$	6 \rightarrow 11
882.9	0.80(7)		$(11^-) \rightarrow 9^-$	8
889.1	1.3(3)	1.39(10)	$14^+ \rightarrow 12^+$	3 \rightarrow 2
889.6	15.7(8)	1.36(3)	$14^+ \rightarrow 12^+$	yrast
892.0	1.0(3)	1.3(2)	$16^+ \rightarrow 14^+$	4
895.6	1.5(1)	1.46(11)	$14^- \rightarrow 12^-$	11
897.3	2.3(2)	1.30(8)	$12^- \rightarrow 10^-$	6
899.7	4.6(2)	1.13(7)	$4^- \rightarrow 4^+$	7 \rightarrow yrast
900.5	0.30(3)	0.67(7)	$14^- \rightarrow 13^-$	9 \rightarrow 5
904.0	0.90(7)	0.73(7)	$13^- \rightarrow 12^+$	5 \rightarrow yrast
908.1 ^c	0.9(2)			
910.7	1.7(1)	1.3(2)	$17^- \rightarrow 15^-$	10
911.2	0.26(6)		$14^+ \rightarrow 12^+$	2
915.5	0.44(6)	1.40(14)	$14^- \rightarrow 14^+$	9 \rightarrow yrast
928.5	0.5(1)		$14^+ \rightarrow 12^+$	2
930			$\rightarrow 18^-$	9
932.7	2.0(5)	1.5(2)	$20^+ \rightarrow 18^+$	yrast
935.1	8.0(4)	1.32(6)	$8^+ \rightarrow 6^+$	$\gamma \rightarrow$ yrast
938.1	1.5(2)	1.40(13)	$10^+ \rightarrow 8^+$	$\rightarrow \gamma$
938.3	0.9(2)	1.36(12)	$16^- \rightarrow 14^-$	11
944.0	1.7(2)	1.37(14)	$19^- \rightarrow 17^-$	5
948.6	1.7(2)	1.39(12)	$12^+ \rightarrow 10^+$	2
965.8	1.8(2)	1.37(11)	$12^+ \rightarrow 10^+$	2
969.7	2.5(3)	0.89(5)	$7^- \rightarrow 6^+$	10 \rightarrow yrast
971.6	3.2(1)	1.38(7)	$13^- \rightarrow 11^-$	\rightarrow 5
992.3	14.2(7)	0.77(4)	$5^- \rightarrow 4^+$	5 \rightarrow yrast
1005.3	0.5(1)	1.6(3)	$10^+ \rightarrow 8^+$	\rightarrow yrast
1013.5	3.2(2)	1.34(11)	$6^+ \rightarrow 4^+$	$\gamma \rightarrow$ yrast
1022.7	0.35(7)		$(19^+) \rightarrow 17^+$	1
1030.4	4.0(3)	1.39(4)	$16^+ \rightarrow 14^+$	yrast
1032.0	7.0(10)	1.36(6)	$2^+ \rightarrow 0^+$	$\gamma \rightarrow$ yrast
1042.7	0.80(10)	1.22(12)	$13^- \rightarrow 11^-$	\rightarrow 5
1046.7	4.4(3)	1.00(9)	$3^+ \rightarrow 2^+$	$\gamma \rightarrow$ yrast
1053.1	0.45(8)	1.45(10)	$12^+ \rightarrow 10^+$	3 \rightarrow
1066	0.28(5)		$(14^+) \rightarrow 12^+$	2
1066.7	0.6(2)	0.6(2)	$15^+ \rightarrow 14^+$	\rightarrow yrast
1068.7	0.8(2)	0.4(1)	$13^+ \rightarrow 12^+$	\rightarrow yrast
1076.2	0.50(5)	1.3(2)	$10^+ \rightarrow 8^+$	$\rightarrow \gamma$
1080.7	0.20(5)		$12^+ \rightarrow 12^+$	3 \rightarrow yrast

TABLE I. (*Continued*).

E_γ ^a	I_γ	R ^b	Spin assignment	Band
1083	0.22(6)		$(14^+) \rightarrow 12^+$	2
1090.4	0.30(3)	0.64(6)	$12^+ \rightarrow 11^+$	3 \rightarrow
1098.5	<0.2		$(5^+) \rightarrow 4^+$	$\gamma \rightarrow$ yrast
1113.5	7.2(4)	1.25(11)	$6^+ \rightarrow 4^+$	$\gamma \rightarrow$ yrast
1118.8	0.72(5)	1.35(9)	$18^+ \rightarrow 16^+$	yrast
1143.0	0.5(7)	1.2(2)	$10^+ \rightarrow 8^+$	\rightarrow yrast
1169.3	2.5(2)	1.42(14)	$14^+ \rightarrow 12^+$	$\gamma \rightarrow$ yrast
1190.3	0.90(8)	1.20(11)	$(8^+) \rightarrow 6^+$	\rightarrow yrast
1265.3	5.8(3)	1.40(9)	$4^+ \rightarrow 2^+$	$\gamma \rightarrow$ yrast
1312	0.33(5)		$\rightarrow 4^+$	\rightarrow yrast
1328.3	0.40(5)	0.9(2)	$15 \rightarrow 14^+$	\rightarrow yrast
1695.1	0.20(6)		$11^+ \rightarrow 10^+$	3 \rightarrow yrast

^aTransition energies given with a decimal are accurate to 0.1 keV, otherwise accurate to 0.5 keV.

^bFor known stretched quadrupole and dipole transitions angular distribution ratios of about 1.4 and 0.8 were obtained.

^cFeeds band 6 through the 603.4 keV transition.

$143^\circ)/I_\gamma(79^\circ \text{ or } 101^\circ)$ angular distribution ratios. For the details of the present method, see [17]. A sample of background-subtracted coincidence spectra for ^{132}Ba is shown in Fig. 1.

The level scheme of ^{132}Ba as obtained in the present work is shown in Fig. 2 in two parts. The first part shows the positive-parity states, and the second part the negative-parity states. Our level scheme contains about 90 new transitions when compared with the level scheme of [14]. It mostly confirms the previous findings reported in [14,18,19]. Some differences arise in a comparison of the level scheme of [14], which are discussed below together with the additions to the previous level scheme.

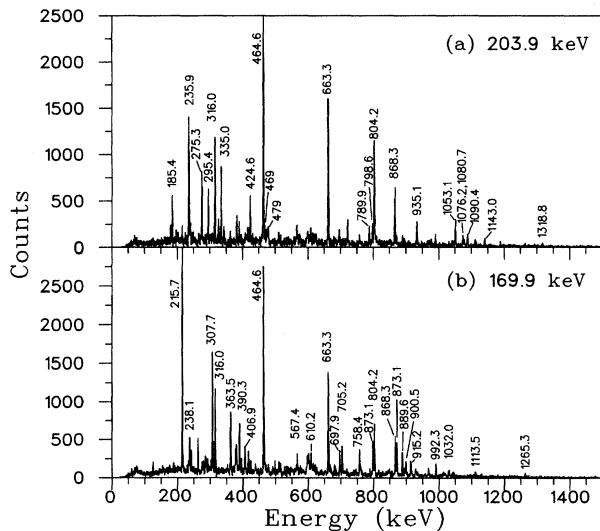


FIG. 1. Sample background-subtracted coincidence spectra for the nucleus ^{132}Ba recorded with NORDBALL, and using the reaction $^{124}\text{Sn}(^{13}\text{C},5n)$ at a beam energy of 65.5 MeV. The spectra are labeled by the gating transition, and the most prominent γ rays are indicated.

Previously, only the 1511 keV 3^+ state was known in the odd-spin sequence of the γ band. In the present work, this branch was observed tentatively up to $I^\pi=(7^+)$. In the even-spin sequence the 723.3 keV transition feeding the 4362 keV 12^+ state is new. Band 1 is the same as reported in [14], except that we add one transition. The 734.6 keV linking transitions to the yrast band has a very small R ratio which implies $I^\pi=15^+$ for the bandhead. The yrast band was established up to $I^\pi=20^+$.

Our finding regarding the decay out of band 3 differs from the previous level scheme [14]. In the present level scheme, this band is connected to other structures by nearly ten transitions and as a result it is placed about 1 MeV higher in energy. The spectrum gated on the 203.9 keV transition in Fig. 1 shows some of the decay paths out of this band. The measured R ratios of the connecting transitions together with those for band 2 unambiguously determine the bandhead spin and parity to $I^\pi=11^+$. In band 2, only the 798.6 and 948.6 keV transitions were known prior to this work.

A 789.9 keV transition feeding the lowest-lying 10^+ state has been reported earlier. In addition, we have observed a complex structure labeled band 4. The three lowest transitions (789.9 keV, 783.1 keV, and 798.3 keV) are clearly of $\Delta I=1$ character, while the higher-lying 671.4, 686.4, and 892.0 keV transitions are most likely of stretched quadrupole type.

It should be noted that as many as four 10^+ states and six 12^+ states are located within ~ 1.0 MeV above the yrast 10^+ and 12^+ states, respectively.

In the negative-parity part of the level scheme two distinct bands, bands 5 and 10, are similar to those in [14], except that in band 5 we have reversed the ordering of the 462.4 and 758.4 keV transitions due to an observation of the 904.0 keV $13^- \rightarrow 12^+$ transition to the yrast band. Our increased sensitivity has resulted in the addition of $\Delta I=2$ cascades, which constitute bands 6, 7, 8, and 11. Bands 5–8 are interconnected by many $\Delta I=1$ transitions, whereas band 11 is only connected to band 10. The 6^- member of band 6 at 2358 keV also feeds the 2313 keV 5^- state assigned to band 8.

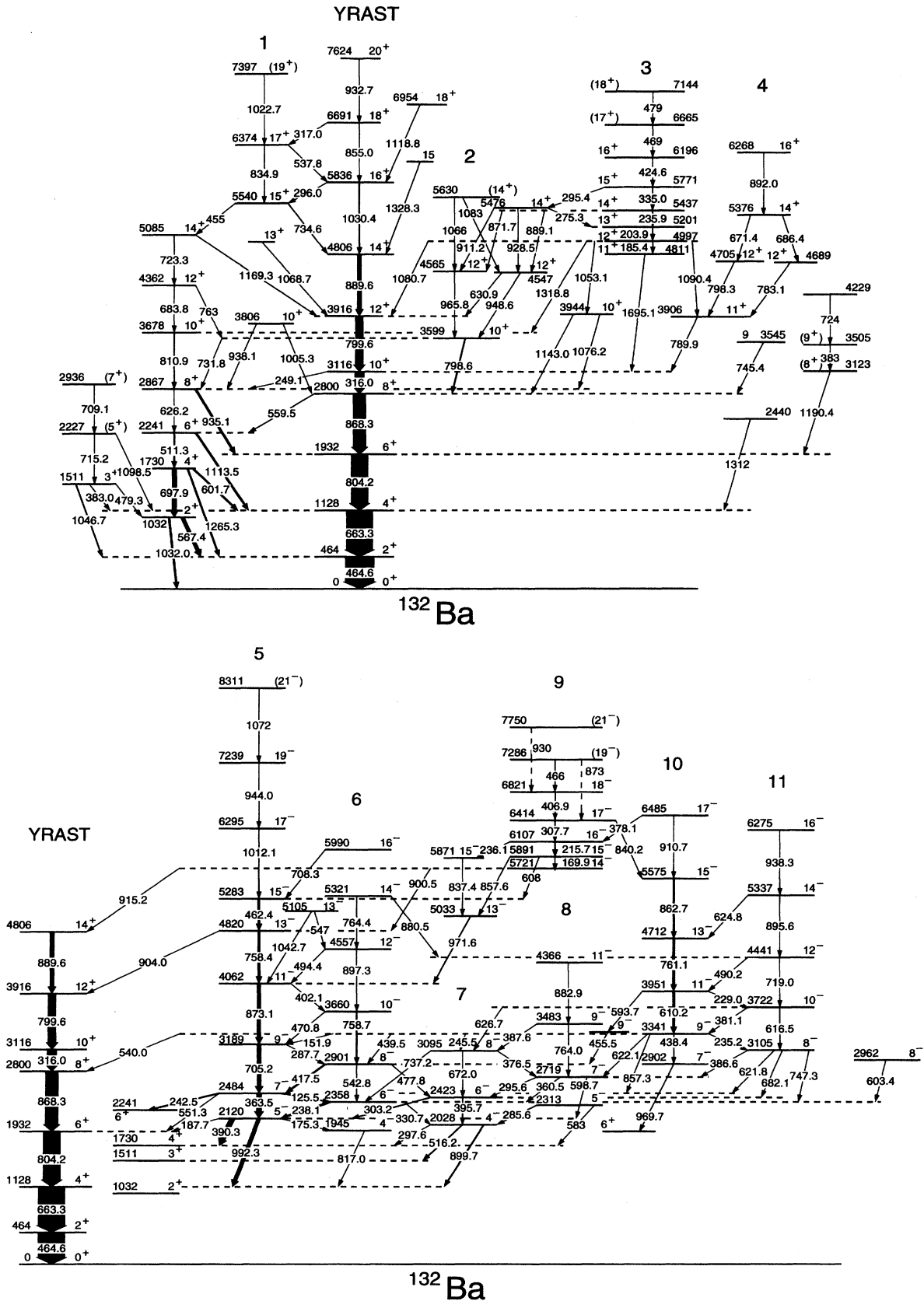


FIG. 2. Level scheme of ^{132}Ba obtained in the present study. The widths of the arrows are proportional to the γ -ray intensity.

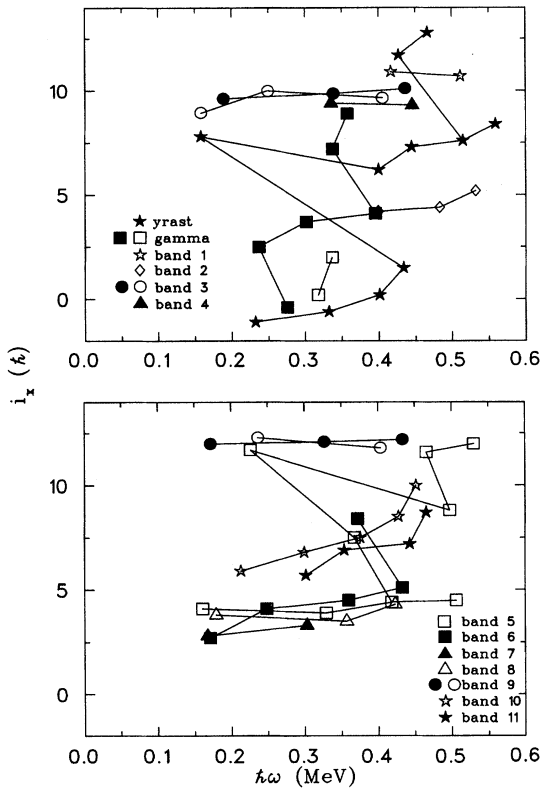


FIG. 3. Experimental alignments in ^{132}Ba . A reference with the Harris parameters $J_0 = 10\hbar^2/\text{MeV}$ and $J_1 = 20\hbar^4/\text{MeV}^3$ has been subtracted. The following values of the K -quantum number were used: $K=0$ for bands 1, 2, 4 and the yrast band; $K=2$ for the γ band and bands 10 and 11; $K=3$ for bands 5–8; $K=7$ for bands 3 and 9.

However, the 45 keV feeding transition could not be observed due to its low energy. The coincidence intensities indicate that the total intensity of this transition is about 1/3 of the 238.1 keV transition intensity.

For band 9 there is a discrepancy with [14] in the feeding-out pattern similar as for band 3 discussed above. We place this band about 1 MeV higher in energy. Band 9 is connected to band 10 via a 840.2 keV transition. It was found that there are more connections between these bands. However, additional linking transition could not be identified. An $I^\pi = 14^-$ assignment for the bandhead is consistent with the measured R ratios and feeding patterns. It should be noted that this band feeds both the negative-parity structures and the positive-parity yrast band.

III. DISCUSSION

The observed level structures of ^{132}Ba have been interpreted by comparing them with the neighboring even-mass nuclei. The rotational properties of the observed bands are discussed below in terms of the cranked shell model (CSM) [20]. Plots of the experimental aligned angular momenta are shown in Fig. 3. A reference given by the Harris parameters $J_0 = 10\hbar^2/\text{MeV}$ and $J_1 = 20\hbar^4/\text{MeV}^3$ has been used to describe the rotating core. This reference gives a reasonable

alignment for the yrast band in ^{132}Ba both below and above the first $h_{11/2}$ neutron alignment.

A. Decoupled positive-parity sequences

The ground-state band of ^{132}Ba can easily be identified up to the 6^+ state. Above that two close-lying 8^+ states are observed. The $B(E2)$ rate of the 868.3 keV $8_1^+ \rightarrow 6_1^+$ transition is about twice as large as the rate for the 559.5 keV $8_1^+ \rightarrow 6_\gamma^+$ transition. The 2800 keV level is therefore most likely the member of the ground-state band.

The smooth behavior of the yrast band is interrupted by a low-lying 10^+ state with about 12 ns [14,21] half-life. This state has been associated with the $\nu h_{11/2}^2$ configuration forming the band head of the S band. The small $B(E2)$ values of the 249.1 and 316.0 keV transitions indicate that neither one of the populated 8^+ states is a member of the neutron S band. As can be seen from Fig. 3, the yrast sequence experiences a band crossing at a rotational frequency of about 0.34 MeV, with an alignment gain of about $7\hbar$. This alignment behavior is very similar to that in the $Z-2$ isotope ^{130}Xe [22], while in the $Z+2$ isotope ^{134}Ce the alignment pattern in the ground-state band is somewhat different [9,23].

Above the 16^+ state in ^{132}Ba the yrast sequence seems to experience another band crossing at a rotational frequency of 0.46 MeV, with a gain of about $5\hbar$. An unexpected feature of this nucleus is the appearance of 15^+ , 17^+ , and 19^+ states, which are connected by $\Delta I=1$ transitions to the yrast band. A similar level structure has recently been observed also in the irregular band built on the isomeric 10^+ state in ^{134}Ce [23], as well as in ^{133}Ba in the band on top of the isomeric $19/2^+$ state, the configuration of which includes a pair of $h_{11/2}$ neutrons [17].

Total Routhian surfaces (TRS's) based on a Woods-Saxon potential have been constructed for ^{132}Ba ; see [24] for details. In the vacuum configuration the surface has three very shallow minima around $\beta_2 \approx 0.15$ at $\gamma \approx -88^\circ$, -28° , and 25° . The minimum at $\gamma = -28^\circ$ becomes favored with increasing rotation. After an $h_{11/2}$ alignment the shape with $\beta_2 \approx 0.15$, $\gamma \approx -80^\circ$ becomes favored. The predicted alignment frequency of $\hbar\omega = 0.21$ MeV is clearly too low when compared with the experimental frequency. In the TR surfaces the $\nu h_{11/2}^2 \pi h_{11/2}^2$ configuration, with a minimum at $\beta_2 \approx 0.15$, $\gamma \approx -30^\circ$, crosses the neutron S band at a frequency of about 0.5 MeV, thereby giving a possible explanation for the observed second alignment gain in the yrast band. Alternatively, the observed alignment gain could be due to the $g_{7/2}$ protons, which also are expected to align around $\hbar\omega = 0.5$ MeV with a minimum at $\beta_2 = 0.12$ and $\gamma \approx -50^\circ$ in the TR surfaces. Band 1 might represent a similar $\pi d_{5/2} g_{7/2} \nu h_{11/2}^2$ configuration.

The proton S band has been observed in the light Ba nuclei up to ^{130}Ba [15]. Also in ^{131}Ba , the proton $h_{11/2}$ alignment has been observed [25]. According to the systematics, the 10^+ state of the proton S band should be found in ^{132}Ba at an excitation energy of about 4 MeV. Although the 10^+ state was not observed in band 4 and there are only two transitions in the band, this band is the best candidate for the proton S band in the present level scheme. Band 4 crosses the ground-state band at $\hbar\omega \approx 0.43$ MeV and the alignment gain is about $9\hbar$. Both of these values agree with those ex-

tracted for the proton S band in lighter Ba nuclei and with the TRS calculations for ^{132}Ba .

Taking the 965.8 and 1066 keV transitions as band members in the level structure labeled band 2, a crossing with the ground-state band at $\hbar\omega = 0.42$ MeV results, with a gain of about $4\hbar$ in aligned angular momentum. These states may belong to a band due to the alignment of the second and the third (or the first and the fourth) $h_{11/2}$ neutrons. Such a picture is supported by an observation of a similar crossing in the $h_{11/2}$ band of ^{131}Ba [25].

The level structure labeled as the γ band is much more irregular than in the neighboring ^{130}Ba nucleus [11]. In ^{132}Ba there is a clear alignment gain, particularly in the even-spin sequence, at low frequencies. Shell model calculations performed for ^{130}Xe [22] predict the proton $d_{5/2}g_{7/2} 6^+$ state to be at 2.1 MeV. Therefore, the irregularity in the γ band could be due to this proton configuration. The plot in Fig. 3 reveals a further alignment gain around $\hbar\omega \approx 0.37$ MeV, which may be due to the alignment of $h_{11/2}$ neutrons.

B. Decoupled negative-parity sequences

On the negative-parity side bands 5–8 form a complicated level structure with many interband transitions. Some of the states in these bands have been observed earlier and have been assigned to neutron configurations [14]. By coupling the lowest $h_{11/2}$ neutron orbital with the lowest positive-parity neutron orbital, four bands are obtained. Bands 5 – 8 most likely represent such a set of bands. In this mass region, the lowest positive-parity one-quasineutron configuration has a mixed $s_{1/2}$ and $d_{3/2}$ character. The similarity of these bands is also evident from the alignment plot of Fig. 3. All of these bands have alignments of $(3-4)\hbar$ at low rotational frequencies. Band 5 experiences a band crossing at a frequency of 0.37 MeV with an alignment gain of about $6\hbar$. Above the band crossing the band becomes irregular. In band 6, we observe an alignment gain at about the same frequency as in band 5. The crossing frequency in bands 5 and 6 is only slightly higher than in the ground-state band, although the first neutron $h_{11/2}$ alignment is blocked in these bands.

Band 10 with a 9^- bandhead has previously been associated with a proton configuration [14]. The 9^- state at 3341 keV feeds several 7^- states. The 438.4 keV stretched quadrupole transition is favored when comparing with the transitions of the same multipolarity to bands 6 and 7. Therefore, the 2902 keV state could belong to band 10. Since bands 10 and 11 are interconnected by $\Delta I=1$ transitions, they are likely to be signature partners. The observation of the unfavored partner makes it possible to test the configuration assignment. These bands have larger initial alignments than the two-quasineutron bands 5 – 8. Bands 10 and 11 are most likely built by coupling the favored signature of the proton $h_{11/2}$ configuration with the favored and unfavored signatures, respectively, of the $g_{7/2}$ configuration. This is supported by the comparison with the ^{133}La nucleus [27]. The sum of alignments of the proton $h_{11/2}$ and $g_{7/2}$ bands in ^{133}La is very close to that extracted in band 10 and 11. Also, the energy splitting between bands 10 and 11 (140 keV at $\hbar\omega = 0.4$ MeV) is comparable to the signature splitting in the $g_{7/2}$ band of ^{133}La [27]. It is evident from Fig. 3 that the alignment starts to increase more rapidly above the fre-

quency of $\hbar\omega = 0.4$ MeV, which could be a sign of the neutron $h_{11/2}$ alignment.

TRS calculations suggest a shape with a large negative γ ($\gamma \approx -85^\circ$) for the lowest negative-parity neutron bands. This shape is favorable for the $h_{11/2}$ neutron alignment, thus explaining the low band-crossing frequency extracted for bands 5 and 6 [14]. For the two-quasiproton bands a shape with a positive γ ($\gamma \approx 30^\circ$) is suggested by TRS calculations, resulting in delayed neutron $h_{11/2}$ alignments.

C. High- K bands

Bands 3 and 9 consist of intense $\Delta I=1$ transitions and the stretched quadrupole cross over transitions are mostly too weak to be observed. Bands showing properties similar to those of bands 3 and 9 are one of the typical features in this mass region. Such bands are believed to be built on configurations involving high- j protons and neutrons coupled to high K and to possess an oblate shape [26].

Based on the excitation energies, bands 3 and 9 are proposed to have four-quasiparticle configurations. We associate bands 3 and 9 with the $\nu h_{11/2} d_{3/2} \pi h_{11/2} g_{7/2}$ and $\nu h_{11/2}^2 \pi h_{11/2} g_{7/2}$ configurations, in line with the configuration assignments of similar bands in this mass region [14,26,28]. These configuration assignments are supported in ^{132}Ba by the bandhead energy arguments, with new placements of the bands. Also, a band with $I^\pi = 29/2^-$ bandhead, very similar to band 9, has recently been observed in ^{133}Ba [17]. This band has been assigned to the $\nu s_{1/2} h_{11/2}^2 \pi h_{11/2} g_{7/2}$ configuration.

The proposed configurations could give rise to high- K bands near collective oblate and collective prolate shapes. At an oblate shape the protons are coupled to high K , while the neutrons have a low K value. At a prolate shape the roles of the protons and neutrons are interchanged. The alignment in band 3 is about $10\hbar$, while in band 9 it is about $12\hbar$, as shown in Fig. 3. To calculate the alignment, $K=7$ was assumed. In both bands the extracted alignment is as large as the sum of alignments of the bands built on the associated proton and neutron two-quasiparticle configurations. This is somewhat surprising, since the proton and neutron bands (for example, bands 10 and 5) are assumed to possess very different shapes. On the other hand, the alignments in bands 3 and 9 are consistent with those extracted for the $\nu h_{11/2} \pi h_{11/2} g_{7/2}$ and $\nu s_{1/2} h_{11/2}^2 \pi h_{11/2} g_{7/2}$ bands in ^{133}Ba [17]. TR surfaces calculated for the configurations proposed in bands 3 and 9 show minima at $\beta_2 = 0.14 - 0.17$ around $\gamma \approx -85^\circ$, $\gamma \approx -30^\circ$, and $\gamma \approx 30^\circ$. These minima are shallow and none of them is clearly favored.

IV. SUMMARY

Excited states of ^{132}Ba have been studied using ^{13}C -induced reactions and the NORDBALL detector array. In all, 11 bands were observed. Five of them were previously unknown. The neutron $h_{11/2}$ configuration was found to play dominant role in the structure of the bands. Several bands show an $h_{11/2}$ alignment at a rotational frequency of about 0.35 MeV. Some evidence was also found for the proton

$h_{11/2}$ alignment. In the TR surfaces the neutron $h_{11/2}$ configuration favors a shape with $\gamma \approx -85^\circ$, whereas the proton $h_{11/2}$ configuration drives the nucleus to $\gamma \approx 30^\circ$. Two of the observed bands consist of dipole transitions. These bands were interpreted to arise from configurations involving both $h_{11/2}$ neutrons and protons.

ACKNOWLEDGMENTS

This work was partially supported by the Academy of Finland, the Danish and Swedish Natural Science Research Councils, and the NORDBALL Collaboration. We are grateful to the staff of the Tandem Accelerator Laboratory at NBI for providing excellent beams and technical support.

-
- [1] J. Blomqvist, in Proceedings of the 4th International Conference on Nuclei far from Stability, Helsingør, Denmark, 1981, (unpublished), p. 536.
- [2] T. Björnstad, M.J.G. Borge, J. Blomqvist, R.D. von Dincklage, G.T. Ewan, P. Hoff, B. Jonson, K. Kawade, A. Kerek, O. Klepper, G. Lövhöiden, S. Mattsson, G. Nyman, H.L. Ravn, G. Rudstam, K. Sistemich, O. Tengblad, and the ISOLDE Collaboration, Nucl. Phys. **A453**, 463 (1986).
- [3] P. van Nes, W.H.A. Hesselink, W.H. Dickhoff, J.J. van Ruyven, M.J.A. de Voigt, and H. Verheul, Nucl. Phys. **A379**, 35 (1982).
- [4] R.E. Shroy, A.K. Gaigalas, G. Schatz, and D.B. Fossan, Phys. Rev. C **19**, 1324 (1977).
- [5] D.R. LaFosse, D.B. Fossan, J.R. Hughes, Y. Liang, P. Vaska, M.P. Waring, and J.-y. Zhang, Phys. Rev. Lett. **69**, 1332 (1992).
- [6] M. Gai, D.M. Gordon, R.E. Shroy, D.B. Fossan, and A.K. Gaigalas, Phys. Rev. C **26**, 1101 (1982).
- [7] A. Kerek, A. Luukko, M. Grecescu, and J. Sztarkier, Nucl. Phys. **A172**, 603 (1971).
- [8] M.B. Goldberg, C. Broude, E. Dafni, A. Gelberg, J. Gerber, G.J. Kumbartzki, Y. Niv, K.-H. Speidel, and A. Zemel, Phys. Lett. **97B**, 351 (1980).
- [9] A. Zemel, C. Broude, E. Dafni, A. Gelberg, M.B. Goldberg, J. Gerber, G.J. Kumbartzki, and K.-H. Speidel, Nucl. Phys. **A383**, 165 (1982).
- [10] T. Morek, H. Beuscher, B. Bochev, D.R. Haenni, R.M. Lieder, T. Kutsarova, M. Müller-Veggian, and A. Neskakis, Z. Phys. A **298**, 267 (1980).
- [11] X. Sun, D. Bazzacco, W. Gast, A. Gelberg, U. Kaup, K. Schiffer, A. Dewald, R. Reinhardt, K.O. Zell, and P. von Brentano, Nucl. Phys. **A436**, 506 (1985).
- [12] J. P. Martin, V. Barci, H. El-Samman, A. Gizon, J. Gizon, W. Klamra, B.M. Nyakò, F.A. Beck, Th. Byrski, and J.C. Merdinger, Nucl. Phys. **A489**, 169 (1988).
- [13] D. Ward, V.P. Janzen, H.R. Andrews, D.C. Radford, G.C. Ball, D. Horn, J.C. Waddington, J.K. Johansson, F. Banville, J. Gascon, S. Monaro, N. Nadon, S. Pilotte, D. Prevost, P. Taras, and R. Wyss, Nucl. Phys. **A529**, 315 (1991).
- [14] E.S. Paul, D.B. Fossan, Y. Liang, R. Ma, and N. Xu, Phys. Rev. C **40**, 1255 (1989).
- [15] R. Wyss, A. Grandérath, R. Bengtsson, P. von Brentano, A. Dewald, A. Gelberg, A. Gizon, J. Gizon, S. Harissopoulos, A. Johnson, W. Lieberz, W. Nazarewicz, J. Nyberg, and K. Schiffer, Nucl. Phys. **A505**, 337 (1989).
- [16] B. Herskind, Nucl. Phys. **A447**, 395c (1985).
- [17] S. Juutinen, P. Šimeček, P. Ahonen, M. Carpenter, C. Fahlander, J. Gascon, R. Julin, A. Lampinen, T. Lönnroth, J. Nyberg, A. Pakkanen, M. Piiparinen, K. Schiffer, G. Sletten, S. Törmänen, and A. Virtanen, Phys. Rev. C **51**, 1699 (1995).
- [18] J. Gizon, A. Gizon, and D.J. Horen, **A252**, 509 (1975).
- [19] C. Flaum, D. Cline, A.W. Sunyar, O.C. Kistner, Y.K. Lee, and J.S. Kim, Nucl. Phys. **A264**, 291 (1976).
- [20] R. Bengtsson and S. Frauendorf, Nucl. Phys. **A314**, 27 (1979); **A327**, 139 (1979).
- [21] A. Dewald, S. Harissopoulos, G. Böhm, A. Gelberg, K.P. Schmittgen, R. Wirowski, Z.O. Zell, and P. von Brentano, Phys. Rev. C **37**, 289 (1988).
- [22] T. Lönnroth, J. Hattula, H. Helppi, S. Juutinen, K. Honkanen, and A. Kerek, Nucl. Phys. **A431**, 256 (1984).
- [23] J. Gascon, J. Nyberg, M. Carpenter, D. Jerrestam, N. Gjørup, A. Johnson, J. Jongman, A. Maj, G. Sletten, P. Tjóm, and R. Wyss, Report on the Research Activities at the Niels Bohr Institute and Nordita, 1989 (unpublished), p. 88.
- [24] R. Wyss, J. Nyberg, A. Johnson, R. Bengtsson, and W. Nazarewicz, Phys. Lett. B **215**, 211 (1988).
- [25] R. Ma, Y. Liang, E.S. Paul, N. Xu, D.B. Fossan, L. Hildingsson, and R.A. Wyss, Phys. Rev. C **41**, 717 (1990).
- [26] E.S. Paul, D.B. Fossan, Y. Liang, R. Ma, N. Xu, R. Wadsworth, I. Jenkins, and P.J. Nolan, Phys. Rev. C **41**, 1576 (1990).
- [27] L. Hildingsson, W. Klamra, Th. Lindblad, C.G. Linden, G. Sletten, and G. Székely, Z. Phys. A **338**, 125 (1991).
- [28] R. Ma, E.S. Paul, D.B. Fossan, Y. Liang, N. Xu, R. Wadsworth, I. Jenkins, and P.J. Nolan, Phys. Rev. C **41**, 2624 (1990).